

# 1 SimSphere Model Sensitivity Analysis Towards Establishing 2 its Use for Deriving Key Parameters Characterising Land 3 Surface Interactions

4  
5 **G. P. Petropoulos<sup>1</sup>, H. M. Griffiths<sup>1</sup>, T. N. Carlson<sup>2</sup>, P. Ioannou-Katidis<sup>1</sup>, T.  
6 Holt<sup>1</sup>**

7 [1] Department of Geography and Earth Sciences, Aberystwyth University, Aberystwyth, SY23  
8 2DB, United Kingdom

9 [2]Department of Meteorology, Pennsylvania State University, University Park, PA 16802,  
10 United States

11  
12 Correspondence to G.P. Petropoulos ([george.petropoulos@aber.ac.uk](mailto:george.petropoulos@aber.ac.uk))  
13

## 14 **Abstract**

15 Being able to accurately estimate parameters characterising land surface interactions is currently  
16 a key scientific priority due to their central role in the Earth's global energy and water cycle. To  
17 this end, some approaches have been based on utilising the synergies between land surface  
18 models and Earth Observation (EO) data to retrieve relevant parameters. One such model is  
19 SimSphere, the use of which is currently expanding, either as a stand-alone application or  
20 synergistically with EO data. The present study aims at exploring the effect of changing the  
21 atmospheric sounding profile on the sensitivity of key variables predicted by this model  
22 assuming different probability distribution functions (PDFs) for its inputs/outputs. To satisfy this  
23 objective and to ensure consistency and comparability to analogous studies conducted previously  
24 on the model, a sophisticated, cutting edge sensitivity analysis (SA) method adopting Bayesian  
25 theory is implemented herein on SimSphere. Our results did not show dramatic changes in the  
26 nature or ranking of influential model inputs in comparison to previous studies. Model outputs  
27 examined using SA were sensitive to a small number of the inputs; a significant amount of first  
28 order interactions between the inputs was also found, suggesting strong model coherence.  
29 Results obtained suggest that the assumption of different PDFs for the model inputs/outputs did  
30 not have an important bearing on mapping the most responsive model inputs and interactions,  
31 but only the absolute SA measures. This study extends our understanding of SimSphere's  
32 structure and further establishes its coherence and correspondence to that of a natural system's

33 behaviour. Consequently, the present work represents a significant step forward in the efforts  
34 globally on SimSphere verification, especially those focusing on the development of global  
35 operational products from the synergy of SimSphere with EO data.

36

## 37 **1 Introduction**

38 Understanding the natural processes of the Earth as well as how the different components (*i.e.*  
39 *lithosphere hydrosphere, the biosphere and atmosphere*) of the Earth's systems interplay,  
40 especially in the context of global climate change, has been recognised by the global scientific  
41 community as a very urgent and important research direction requiring further investigation  
42 (Battrick et al. 2006). This requirement is also of crucial importance for addressing directives  
43 such as the EU Water Framework Directive. To this end, being able to accurately estimate  
44 spatio-temporal estimates of parameters such as the latent (LE) and sensible (H) heat fluxes as  
45 well as of soil moisture is of great importance. This is due to their important role in many  
46 physical processes characterising land surface interactions of the Earth system as well as their  
47 practical use in a wide range of multi-disciplinary studies and applications (Kustas and  
48 Anderson, 2009; Seneviratne et al. 2010).

49 As a result, deriving information on the spatio-temporal distribution of these parameters has  
50 attracted the attention of scientists from many disciplines. Over the past few decades, a wide  
51 variety of approaches for their retrieval have been proposed operating at different observation  
52 scales, including datasets from ground instrumentation, simulation models and Earth  
53 Observation (EO). Recent studies have also focused on exploring the synergies between EO data  
54 and land surface process models (see reviews by Olioso, 1992 and **Petropoulos**, 2013).  
55 Essentially, these techniques endeavour to provide improved predictions by combining the  
56 horizontal coverage and spectrally rich content of EO data with the vertical coverage and  
57 excellent temporal resolution of simulation process models.

58 One such group of approaches, so-called the “triangle” method (Carlson, 2007), is used to  
59 predict regional estimates of LE, H fluxes and soil moisture content (SMC). SimSphere is a Soil  
60 Vegetation Atmosphere Transfer (SVAT) model, originally developed by Carlson and Boland  
61 (1978) and considerably modified to its current state by Gillies et al. (1997) and **Petropoulos** et  
62 al. (2013a). SVAT models are essentially mathematical representations of 1-dimensional ‘views’  
63 of the physical mechanisms controlling energy and mass transfers in the  
64 soil/vegetation/atmosphere continuum, providing deterministic estimates of the time course of

65 various variables characterising land surface interactions at time-steps appropriate to the  
66 dynamics of atmospheric processes (Olioso et al., 1999). An overview of SimSphere use was  
67 recently provided by Petropoulos et al. (2009a). The different facets of the SVAT model's  
68 overall structure, namely the physical, the vertical and the horizontal, are illustrated in Figure 1  
69 (left). An extensive mathematical description of the model can be found in Carlson and Boland  
70 (1978), Carlson et al. (1981) and Gillies and Carlson (1995). The SimSphere model is  
71 maintained and is distributed freely globally (both the executable version and model code) from  
72 Aberystwyth University, United Kingdom (<http://www.aber.ac.uk/simsphere>).

73 As regards the “triangle” method in particular, it has its foundations in the physical properties  
74 encapsulated in a satellite-derived scatterplot of surface temperature (Ts) and vegetation index  
75 (VI), linked with the SimSphere model. Petropoulos et al. (2009b) have underlined the potential  
76 of this group of approaches for operational implementation in deriving estimates of LE/H fluxes  
77 and/or SMC. A recent description of the “triangle” workings can be found in Petropoulos and  
78 Carlson (2011). At present variants of this method are explored - or even some already  
79 implemented in practice - for deriving, in some cases operationally and on a global scale,  
80 estimates of LE and H fluxes and/or SMC (Chauhan et al., 2003; Piles et al., 2011; ESA STSE,  
81 2012). In addition, SimSphere use is continually expanding worldwide both as an educational  
82 and as a research tool - used either as a stand-alone application or synergistically with EO data -  
83 to conduct studies aiming to improve understanding of land surface processes and their  
84 interactions. Considering the research and practical work with respect to SimSphere use, it is  
85 evidently of primary importance to execute a variety of validity tests to evaluate its adequacy  
86 and coherence in terms of its ability to accurately and realistically represent Earth's surface  
87 processes.

88 Performing a sensitivity analysis (SA) provides an important and necessary validity  
89 component of any computer simulation model or modelling approach before it is used in  
90 performing any kind of analysis. SA allows determining the effect of changing the value of one  
91 or more input variables of a model and observing the consequence that this has on given outputs  
92 simulated by the model. Its implementation on a model allows understanding the model's  
93 behaviour, coherence and correspondence to what it has been built to simulate (Saltelli et al.,  
94 1999; 2000; Nossent et al., 2011). As such, SA provides a valuable method to identify significant  
95 model inputs as well as their interactions and rank them (Chen et al., 2012), offering guidance to  
96 the design of experimental programs as well as to more efficient model coding or calibration.

97 Indeed, by means of a SA unrelated parts of the model may be dropped or a simpler model can  
98 be built or extracted. The latter can reduce, in some cases significantly, the required computing  
99 power while maintaining the models' correspondence to natural system's behaviour to real world  
100 (Holvoet et al., 2005).

101 A range of SA approaches have been proposed, a comprehensive overview of which can be  
102 found for example in Saltelli et al. (2000). One group includes the so-called Global SA (GSA)  
103 methods. These techniques aim to apportion the output variability to the variability of the input  
104 parameters when they vary over their whole uncertainty domain, generally described using  
105 probability densities assigned to the model's inputs. The sensitivity of the input parameters is  
106 examined based on of the use of samples derived directly from the model, which are distributed  
107 across the parameter domain of interest. These methods, despite their high computational  
108 demands, have become popular in environmental modelling due to their ability to incorporate  
109 parameter interactions and their relatively straightforward interpretation (Nossent et al., 2011).  
110 They also account for the influence of the input parameters over their whole range of variation,  
111 which in turn enables obtaining SA results independent of any "modelers' prejudice", or site-  
112 specific bias (Song et al., 2012).

113 Petropoulos et al. (2009a) in a recent review of SimSphere exploitation underlined the  
114 importance of carrying out SA experiments on the model, as part of its overall verification. In  
115 response, Petropoulos et al. (2009c; 2010; 2013a,b,c) performed advanced GSA on SimSphere  
116 based on a Gaussian process emulator. As previous SA studies on SimSphere had been scarce,  
117 their results provided for first time an insight into the model architecture, allowing the mapping  
118 of the sensitivity between the model inputs and key model outputs. Although these studies varied  
119 all the model input parameters across their full range of variation, a particular atmospheric  
120 sounding setting had been used in these GSA experiments by the authors. In addition, the effect  
121 of different probability distribution functions (PDFs) for the model inputs/outputs to the obtained  
122 had not been adequately explored.

123 In this context, the aim of the present study was to perform a GSA on SimSphere using an  
124 atmospheric sounding derived from a different region and evaluate the effect of atmospheric  
125 sounding on the SA results obtained on SimSphere assuming different PDFs for the model  
126 inputs/outputs. This will allow us to extend our understanding of this model structure and further  
127 establishing its coherence.

128

## 129 **2 The Bayesian Sensitivity Analysis method**

130 To satisfy the objectives of this study and to ensure consistency and comparability of our work to  
131 previous studies on SimSphere, SA is conducted here by employing a sophisticated, cutting edge  
132 GSA method adopting on Bayesian Analysis of Computer Code Outputs (BACCO; Kennedy and  
133 O'Hagan, 2001). It is implemented using the GEM-SA software, the development of which was  
134 funded by the National Environmental Research Council, United Kingdom. The theory behind  
135 the BACCO GEM-SA technique can be found by Oakley and O'Hagan (2004); detailed  
136 descriptions of the mathematical principles governing the GP emulation are available in  
137 Kennedy and O'Hagan (2001), Kennedy (2004) and Oakley and O'Hagan (2004). The use of the  
138 Gaussian processes (GP) to model unknown functions in Bayesian statistics dates back to  
139 Kimeldorf & Wahba (1970) and O'Hagan (1978).

140 Briefly, BACCO GEM-SA implementation consists of two phases: First, a statistically-based  
141 representation (i.e. an emulator) of the model is built from training data obtained from  
142 simulations derived from the actual model, which have been designed to cover the multi-  
143 dimensional input space using a space-filling algorithm. Second, the emulator itself is used to  
144 compute a number of statistical parameters to characterise the sensitivity of the targeted model  
145 output in respect to its inputs.

146 BACCO SA implementation starts from a prior belief about the code (i.e. that it has no  
147 numerical error) and then based on a GP model, Bayes' theorem and a set of the model code runs  
148 this assumption is refined, to yield the posterior distribution of the output, which is the emulator.  
149 In building the emulator, the most important prior assumption is that the output emulator is a  
150 reasonably smooth function of its inputs. On this basis, the emulator is used to calculate a mean  
151 function, which attempts to pass through the observed runs and the same time it quantifies the  
152 remaining uncertainty due to the emulator being an approximation to the true code. Within  
153 BACCO, various statistical measures are generated automatically when the emulator is built in  
154 order to check the accuracy of both types of output.

155 In simple mathematical terms, the basic SA output from GEM-SA includes a direct  
156 decomposition of the model output variance into factorial terms, called 'importance measures'  
157 (e.g. Ratto et al., 2001):

158

159 
$$V(Y) = \sum_{i=1}^s D_i + \sum_{i < j} D_{ij} + \dots + D_{1\dots s} \quad (1)$$

160 
$$D_i = V(E(Y|X_i)) \quad (1a)$$

161 
$$D_{ij} = V(E(Y|X_i, X_j)) - V(E(Y|X_i)) - V(E(Y|X_j)) \quad (1b)$$

- 162 -  $s$  denotes the number of inputs (so-called ‘factors’),  
 163 -  $V(Y)$  is the total variance of the output variable  $Y$   
 164 -  $D_i$  is the importance measure for input  $X_i$ ,  
 165 -  $D_{ij}$  is the importance measure for the interaction between inputs  $X_i$  and  $X_j$   
 166 -  $D_{1\dots s}$  denote similar formulae for the higher order terms.  
 167 -  $E(Y|X_i)$  is the conditional expectation of  $Y$  given a value of  $X_i$  and the variance of  
 168  $E(Y|X_i)$  is taken over all inputs factors which are fixed in the conditional expectations.

169 In addition, in the BACCO method, sensitivity indices are computed by dividing the importance  
 170 measures from equation 6 by the total output variance as follows:

171 
$$S_i = \frac{D_i}{V(Y)}, \quad S_{ij} = \frac{D_{ij}}{V(Y)}, \quad (3)$$

172 These ratios  $S_i$  for  $i=1, \dots, s$  are called *main effects* or *first order sensitivity indices*, because each  
 173  $S_i$  delivers a direct measure of the share of the output variance explained by  $X_i$ . The main effect  
 174 or first order sensitivity index  $S_i$  is the expected amount of variance that would be removed from  
 175 the total output variance if the true value of  $X_i$  was known (within its uncertainty range). Thus,  
 176 this is a measure that quantifies the relative importance of an individual input variable  $X_i$ , in  
 177 driving the total output uncertainty, indicating where to direct future efforts to reduce that  
 178 uncertainty. Using similar formulae higher order sensitivity indices (*joint effect indices*) are also  
 179 computed in GEM-SA to compute the sensitivity of the model output to input parameter  
 180 interactions. However, in practice, because the estimation of  $S_i$  or  $S_{ij}$  or higher order can be  
 181 computationally very expensive, the SA is rarely carried out further after the computation of first  
 182 order interaction indices (i.e. the second term of Equation 3 above). This is also the case with  
 183 GEM-SA.

184 Thus, from the definitions of the above indices, and assuming non-correlated inputs, a complete  
 185 series development of the output variance can be achieved:

$$186 \quad \sum_i S_i + \sum_{i < j} S_{ij} + \sum_{i < j < m} S_{ijm} + \dots + S_{12\dots k} = 1 \quad (4)$$

187 where higher order indices are defined in a similar way to Equation 7. This decomposition of  
 188 variance into main effects and interactions is commonly known as *Analysis of Variance-High*  
 189 *Dimensional Model Representation (HDMR)*.

190 The percentage variance contribution of each input's main effect is also reported in BACCO,  
 191 providing a simple means of ranking the inputs in terms of their importance. The percentage  
 192 variance component associated with each input measures the amount its main effect contributes  
 193 to the total output variance, based on the uncertainty distributions for all inputs. It should be  
 194 noted that, in general, summing the main effect contributions will not total to 100 % because of  
 195 the additional contributions from the interaction effects. However, the total can be used to  
 196 determine the degree of interactions.

197 In addition to the above indices, another measure that is computed in GEM-SA is the *total*  
 198 *sensitivity index*. This is used to provide a cheaper computational method of investigating the  
 199 higher order sensitivity effects as it collects all the interactions involving  $X_i$  in one single term.  
 200 The total sensitivity index of a given factor  $X_i$  takes into account the main effect and the effect of  
 201 all its interactions with other model inputs, and is defined as:

$$202 \quad ST_i = \frac{D_i + D_{i,\sim i}}{V(Y)} \quad (5)$$

203 where  $D_{i,\sim i}$  indicates all interactions between factor  $X_i$  and all the others ( $X_{\sim i}$ ).

204 The total sensitivity index represents the expected amount of output variance that would remain  
 205 unexplained (residual variance) if only  $X_i$  were left free to vary over its range, the value of all  
 206 other variables being known. The usefulness of the  $ST_i$  is that it is possible to compute them  
 207 without necessarily evaluating the single indices  $S_i$  (and higher order ones), making the analysis  
 208 computationally affordable. The total sensitivity indices are generally used to identify  
 209 unessential variables (i.e. those that have no importance neither singularly nor in combination  
 210 with others) while building a model. The existence of large total effects relative to main effects  
 211 implies the presence of interactions among model inputs.

212 The BACCO method has already supplied useful insights in various disciplines and in various  
213 SA studies underlying the advantages of this approach (Kennedy and O'Hagan, 2001; Johnson et  
214 al., 2011; Kennedy et al., 2012; Parry et al., 2012). Petropoulos et al (2009c) demonstrated for  
215 the first time the use of the BACCO method in performing a SA on SimSphere, providing an  
216 insight into the model structure. Petropoulos et al. (2010) performed a comparative study of  
217 various emulators including BACCO GEM, investigating the effect of sampling method and size  
218 on the sensitivity of key target quantities simulated by SimSphere. Their results showed that the  
219 sampling size and method did affect the SA results in terms of absolute values, but had no  
220 bearing in identifying the most sensitive model inputs and their interactions, for model outputs  
221 on which SA was performed.

222

### 223 **3 Sensitivity analysis implementation**

224 To ensure consistency and comparability with previous analogous SA studies on SimSphere, the  
225 BACCO GEM-SA was implemented herein along the lines of previous similar GSA studies  
226 applied to that model (Petropoulos et al., 2009c; 2010; 2013a,b,c). The only difference was the  
227 use of a different atmospheric sounding profile derived from a dissimilar location and season.  
228 Thus, the sensitivity of the following SimSphere outputs was evaluated:

- 229 • Daily Average Net Radiation ( $\overline{Rn}_{daily}$ )
- 230 • Daily Average Latent Heat flux, ( $\overline{LE}_{daily}$ )
- 231 • Daily Average Sensible Heat flux ( $\overline{H}_{daily}$ ),
- 232 • Daily Average Tair ( $\overline{Tair}_{daily}$ )
- 233 • Daily Average Surface Moisture Availability ( $\overline{Mo}_{daily}$ ).
- 234 • Daily Average Evaporative Fraction ( $\overline{EF}_{daily}$ )
- 235 • Daily Average Non-Evaporative Fraction ( $\overline{NEF}_{daily}$ )
- 236 • Daily Average Radiometric Temperature ( $\overline{Trad}_{daily}$ ).

237

238 A design space of 400 SimSphere simulations developed using the LP-tau sampling method. In  
239 creating the input space from the 400 model runs, all SimSphere inputs were allowed to vary,  
240 except those of the geographical location (latitude/longitude) and atmospheric profile (Figure 2),



241 for which *a priori* real observations for the August 7<sup>th</sup>, 2002 were used from the Loobos  
242 CarboEurope site, located in The Netherlands (52° 10' 04.29" N, 05° 44' 38.25" E). In  
243 accordance to previous GSA studies on SimSphere, GEM SA was implemented assuming both  
244 normal and uniform probability distribution functions (PDFs) for the inputs/outputs from the  
245 model. For all variables, the theoretical ranges of values were defined from the entire possible  
246 theoretical range which they could take in SimSphere parameterisation (Table 1). The potential  
247 of co-variation between the parameters was assumed negligible, as in previous studies. In  
248 addition, the emulator performance was evaluated based on the “leave final 20 % out” method  
249 offered in GEM-SA, again in accordance to previous GEM SA studies conducted to the model.

250

## 251 **4 Results**

### 252 **4.1 Emulator validation**

253 The uncertainty of the SA due to the performance of the emulator was evaluated on the basis of a  
254 number of statistical measures computed internally by GEM-SA. Those included the “cross  
255 validation root mean square error”, “cross-validation root mean squared relative error” and the  
256 “cross-validation root mean squared standardized error (RMSE)”. In addition a unitless  
257 parameter called “roughness value”, also computed internally in GEM SA, was used. This  
258 parameter provides an estimate of the changes in model outputs in response to changes in the  
259 inputs to the model. Finally, the “sigma-squared” statistical parameter, also computed within  
260 GEM-SA, was also used to statistically appreciate the performance of the emulator build. Within  
261 BACCO GEM-SA, this expresses the variance of the emulator after standardising the output, and  
262 effectively provides a measure of the quality of the fit of the emulator to the original model code.

263 Tables 2 and 3 summarise the results from the computation of the main statistical measures used  
264 to evaluate the performance of the emulator. As can be observed, sigma-squared’ values for all  
265 parameters were low, as were RMSE values for all model outputs. Cross-validation RMSD  
266 varied widely between 3.03 % ( $\overline{Tair_{daily}}$ ) and 41.63 % ( $\overline{H_{daily}}$ ). Roughness values for the  
267 majority of the model inputs were reported having very low values for both normal and uniform  
268 PDFs, indicating that the built emulator is a very good approximation of the actual model. For  
269 thermal inertia, for example, roughness values are 0 for all model outputs with the exception of  
270 H flux and daily LE and H fluxes (which are all 0.01). Most roughness values obtained were  
271 below 1.0, suggesting that the emulator responded smoothly to variations in model inputs.

272 Roughness values above 1.0 were rare (eg. for  $\overline{H_{daily}}$  were vegetation height and surface soil  
273 moisture availability (Mo) and for  $\overline{Trad_{daily}}$  were aspect, fractional vegetation cover, vegetation  
274 height and Mo). Roughness values above one were rare and indicated some degree of non-  
275 linearity between model inputs and outputs. However, these are not significant enough to suggest  
276 an extreme level of non-linear relationships. Noticeably, the results obtained herein in regards to  
277 the emulator accuracy were largely comparable to previous GSA studies on SimSphere  
278 (Petropoulos et al., 2009c; 2013,a,b,c), suggesting a good emulator build, able to emulate the  
279 target quantities examined reasonably accurately.

## 280 4.2 SA results

281 Tables 4 and 5 summarise the relative sensitivity of the model outputs with respect to the model  
282 inputs, for both the cases of normal and uniform PDFs assumptions for the model inputs/outputs.  
283 Input parameters with a main effect  $> 1\%$  and/or  $> 1\%$  total effect are highlighted in grey.  
284 Figure 3 exemplifies the main effect and total effects for each model output of which the SA was  
285 examined. The following sections systematically describe the main results obtained in terms of  
286 the SA for both cases of PDFs assumption, focusing primarily on the analysis of the main and  
287 total SA indices computed.

### 288 4.2.1 Parameter sensitivity for $\overline{Rn_{daily}}$

289 Main effects and total effects ranged from 0 to 50.1 % and 0 to 63.6 %, respectively, for normal  
290 PDFs (Table 4, Figure 3) and from 0 to 48.1 % and 0 to 65.7 % (Table 5), respectively in the  
291 case of uniform PDFs assumption. Under normal PDFs assumption, the inputs with the largest  
292 percentage variance contribution were aspect (50.1 %), slope (20.3 %) and Fr (7.2 %), and LAI  
293 (2.1 %) and Mo (3.6 %) were also relevant. As Table 4 shows, these parameters also contributed  
294 significantly to the total effects, although vegetation height also contributed here (1.2 %).  
295 Clearly, changing the PDFs to uniform did not alter the nature or the ranking of the most  
296 important model inputs (Table 5, Figure 3). Yet, it is noticeable that for this PDFs assumption,  
297 surface roughness input became more important, contributing 1.1 % to the total effects. In  
298 summary, the model input parameters with the highest total effects (i.e. those to which  $\overline{Rn_{daily}}$  is  
299 most sensitive) were aspect, slope, Fr, LAI, Mo, vegetation height and surface roughness. Only  
300 nine significant ( $> 0.1\%$ ) first order interactions were found for this parameter assuming a  
301 normal PDFs and assuming a uniform PDFs for the model inputs. Assuming a uniform PDFs, the

302 most significant first order interactions were between slope and aspect (13.4 %) and between Fr  
303 and LAI (0.6 %). For normal PDFs the interaction between slope and aspect was, by far the most  
304 important (10.20 %). Interactions between aspect and Fr (0.4 %), Fr and LAI (0.3 %) and aspect  
305 and Mo (0.3 %) were also significant.

#### 306 **4.2.2 Parameter sensitivity for $\overline{H_{daily}}$**

307 Main effects and total effects were lower in this case and ranged from 0 to 15.2 % and from 0 to  
308 31.1 %, respectively, for normal PDFs (Table 4) and from 0 to 16.6 % and 0 to 30.4 %, respectively,  
309 respectively, for uniform PDFs (Table 5). Under normal PDFs, the inputs parameters with the  
310 largest percentage variance contribution were Fr (15.2 %), Mo (11.7 %), aspect (10.9 %) and  
311 vegetation height (10.4 %). Surface roughness (3.5 %) and slope (1.4 %) were also important. In  
312 terms of the total effects, aspect was the most important parameter (31.1 %) for the simulation of  
313  $\overline{H_{daily}}$  by the model, followed by vegetation height (29.7 %), Mo (26.3 %) and Fr (25.5 %). A  
314 number of other parameters also showed significant total effects (Table 4). The nature and rank  
315 of significant input parameters to main effects was also not changed by changing the PDFs to  
316 uniform (Table 5, Figure 3). In terms of the total effects, however, vegetation height becomes the  
317 most important by a small margin (30.4 % compared to 30.1 % for aspect). Numerous important  
318 input parameters are seen to influence  $\overline{H_{daily}}$  therefore, the most important being aspect, Fr,  
319 vegetation height, Mo and surface roughness. A large number of first order interactions with  
320 values higher than 0.1% were observed for  $\overline{H_{daily}}$  assuming a uniform PDFs (32 in total) and  
321 assuming a normal PDFs (39 in total). Assuming a uniform PDFs the most important interactions  
322 were between vegetation height and surface roughness (4.76 %), Fr and Mo (2.46 %) and  
323 vegetation height (1.95 %), respectively and between aspect and surface roughness (1.67 %) and  
324 Mo (1.40 %), respectively. The most significant interaction assuming a normal PDFs was  
325 between vegetation height and surface roughness (4.31 %), but interactions between aspect and  
326 surface roughness (2.52 %), Mo (1.71 %), vegetation height (1.13 %) and O<sub>3</sub> in the air (0.72 %) respectively  
327 respectively and between Fr and Mo (2.26 %) and vegetation height (1.91 %) were also found. In  
328 terms of second order or higher interactions, a higher level of significant interactions were found,  
329 with 16.8 % and 21.9 % noted assuming normal and uniform PDFs, respectively.

### 330 **4.2.3 Parameter sensitivity for $\overline{LE}_{daily}$**

331 As regards the  $\overline{LE}_{daily}$ , SA results showed ranges in main effects and total effects ranging from 0  
332 to 36.0 % and 0 to 51.9 %, respectively, for normal PDFs assumption (Table 4) and from 0 to  
333 29.8 % and 0 to 48.0 %, respectively, for uniform PDFs (Table 5, Figure 3). Under normal PDFs,  
334 the model inputs with the highest percentage variance contribution were those of aspect (36.0  
335 %), Mo (17.6 %), Fr (8.1 %), slope (8.0 %) and cuticle resistance (1.0 %). This is also mirrored  
336 in the total effects results obtained, yet at higher percentage contributions (e.g. 51.9 % for the  
337 aspect). Both PSI and substrate maximum volumetric water content contributed > 1 % to the  
338 total effects also. Once again, the nature and rank of significant model input parameters was  
339 mirrored when the PDFs was changed to uniform, but additional parameters contribute to the  
340 total effects, including [Ca], [O<sub>3</sub>] in the air, ground emissivity, RKS, CosbyB, and THM. In  
341 summary, results suggest that the most important model inputs influencing the simulation of  
342  $\overline{LE}_{daily}$  were aspect, Mo, Fr and slope. Assuming uniform PDFs for the model inputs, two first  
343 order interactions dominate for this parameter – those between slope and aspect once more (6.8  
344 %) and those between Fr and Mo (6.8 %). Interactions between aspect and Mo (1.0 %) and Fr  
345 (4.6 %), respectively, are also important. When normal PDFs for model inputs/outputs was  
346 assumed, twenty four first order interactions with values higher than 0.1% were observed, and  
347 once again, the interaction between slope and aspect (6.1 %) were the most important. However,  
348 important interactions between Fr and Mo (4.6 %), aspect and Mo (1.2 %) and between aspect  
349 and Fr (0.8 %) were also observed.

350

### 351 **4.2.4 Parameter sensitivity for $\overline{Trad}_{daily}$**

352 Main effects and total effects for  $\overline{Trad}_{daily}$  simulation by SimSphere ranged from 0 to 34.9 % and  
353 52.0 % respectively, assuming normal PDFs for the model inputs (Table 4, Figure 3) and from 0  
354 to 29.6 % and 49.2 %, respectively for the case of uniform PDFs (Table 5). For normal PDFs the  
355 most important model inputs were aspect (34.9 %), Mo (16.9 %) and slope (12.7 %), with Fr and  
356 vegetation height also important. This is mirrored in the total effects, but here LAI, [O<sub>3</sub>] in the  
357 air, surface roughness, obstacle height and THM also contributed more than 1 %. The nature and  
358 ranking of the model inputs contributing significant main effects under uniform PDFs was  
359 largely similar to that of normal PDFs. In common with the parameters discussed above,

360 therefore, aspect, slopes, Mo and vegetation characteristics (Fr and height) exert the most  
361 influence on  $\overline{Trad}_{daily}$ . Assuming a uniform PDFs twenty one first order interactions with values  
362 higher than 0.1% were reported. The most important was between slope and aspect (9.5 %),  
363 followed by some less important interactions e.g. between Fr and Mo (1.2 %), and between  
364 aspect and Mo (0.8 %). On the other, assuming a normal PDFs twenty four significant first order  
365 interactions with values higher than 0.1% were returned. The two most important were once  
366 again between slope and aspect (8.9 %) and between aspect and Mo (0.9 %). Interactions  
367 between Fr and Mo (0.9 %) and aspect and Fr (0.7 %) were also important. Second order or  
368 higher interactions contributed 5.2 % and 8.0 % in the total variance decomposition for the  
369 normal and uniform PDFs, respectively.

#### 370 **4.2.5 Parameter sensitivity for $\overline{Mo}_{daily}$**

371 For main effects and total effects for normal PDFs, a similar range was observed for  $\overline{Mo}_{daily}$  as  
372 for other parameters, from 0 to 28.5 % and 50.2 %, respectively (Table 4, Figure 3). However, a  
373 much larger range was observed for these values under uniform PDFs – from 0 to 96.4 % and  
374 97.6 % for main and total effects, respectively (Table 5). For normal PDFs the most important  
375 model input parameters were aspect (28.5 %), slope (17.1 %) and LAI (12.0 %) in the main  
376 effects. These were also important in terms of total effects but in addition many other factors also  
377 become important in that case, the most significant being Mo (7.1 %), Fr (6.7 %) and station  
378 height (4.9 %). In this case therefore, although the most significant parameters were, once again,  
379 aspect and slope, many other parameters also appear to contribute to the sensitivity of  $\overline{Mo}_{daily}$ .  
380 Evidently, a marked difference in terms of sensitivity was observed when a uniform PDFs is  
381 assumed for this parameter (Table 5, Figure 3). In this case, the sensitivity is dominated by Mo  
382 in both the main and total effects – 96.4 % and 97.6 %, respectively. In the total effects, substrate  
383 maximum volumetric water content and PSI both contributed to a much lesser degree. For the  
384 case of uniform PDFs, only one first order interaction with values higher than 0.1% was  
385 observed between Mo and substrate maximum volumetric water content (0.2 %). Thirty two first  
386 order interactions with values higher than 0.1% were reported assuming a normal PDFs for the  
387 model inputs/outputs. The interaction between slope and aspect was once again the most  
388 significant (8.5 %), followed by that between Fr and LAI (2.18 %). Interactions between aspect  
389 and LAI (1.4 %) and Mo (1.2 %), respectively, were also important.

#### 390 **4.2.6 Parameter sensitivity for $\overline{Tair_{daily}}$**

391 Ranges of main and total effects for this parameter were found to be comparable to the majority  
392 of the other parameters discussed previously. For normal PDFs these range from 0 to 21.89 %  
393 and from 0 to 43.8 %, respectively (Table 4, Figure 3) and for uniform PDFs these range from 0  
394 to 18.1 % and 0 to 43.8 % (Table 5), respectively. For main effects under normal PDFs the most  
395 significant model input parameters were, once again, aspect (21.9 %), Fr (16.7 %), vegetation  
396 height (7.8 %), surface Mo (7.0 %) and surface roughness (6.5 %). The total effects were  
397 broadly similar, but surface roughness became the third most important parameter, whereas other  
398 inputs (e.g. station height, [O<sub>3</sub>] in the air, obstacle height and PSI) become important. Under  
399 uniform PDFs, the most important parameters were aspect (18.1 %), Fr (16.9 %), Mo (8.2 %),  
400 vegetation height (5.9 %), and surface roughness (4.8 %). Under total effects, once again, surface  
401 roughness becomes more important, and the same additional model parameters as were observed  
402 under normal PDFs also contributed greater than 1 %. Once again, aspect and Fr, vegetation  
403 height and surface roughness seem to be the most important variables influencing  $\overline{Tair_{daily}}$ .

404 Twenty three first order interactions with values higher than 0.1% were found for this  
405 parameter, and once again, the interaction between slope and aspect is the most important (5.2  
406 %), although it is closely followed by interactions between vegetation height and surface  
407 roughness (4.4 %) and between Fr and vegetation height (2.0 %) and between aspect and surface  
408 roughness (1.9 %). Of the twenty three first order interactions higher than 0.1% also found  
409 assuming a normal PDFs for model inputs/outputs, the most important was between slope and  
410 aspect (5.0 %), closely followed by the interactions between vegetation height and surface  
411 roughness (4.1 %) inputs, but a number of other important interactions are evident. These include  
412 interactions between aspect and surface roughness (2.3 %), vegetation height (1.5 %), Fr (1.4 %)  
413 and Mo (0.7 %), respectively and between Fr and vegetation height (1.9 %) and surface  
414 roughness (1.0 %), respectively.

#### 415 **4.2.7 Parameter sensitivity for $\overline{EF_{daily}}$**

416 Once again, the ranges of main and total effects reported for the sensitivity of  $\overline{EF_{daily}}$  were to a  
417 large degree similar to most of the other parameters already discussed. For normal PDFs, main  
418 effects of the inputs ranged widely from 0 to 38.2% and from 0 to 49.5%, respectively (Table 4,  
419 Figure 3) and for the case of uniform PDFs from 0 to 35.7% and from 0 to 49.1%, respectively

420 (Table 5). Mo was found to be the most important model input parameter here in terms of main  
421 effects under normal PDFs (38.2%), followed by Fr (10.4%), vegetation height (8.2%) and  
422 aspect (4.3%). As Table 4 shows, many additional parameters become important contributors to  
423 total effects although the nature and rank of the most significant parameters does not change.  
424 Once again, Table 5 shows very little differences in terms of the nature and ranking of the main  
425 and total effects under a uniform PDFs assumption for the model inputs/outputs. Therefore, for  
426 this parameter, the most important model input parameters are Mo, Fr, vegetation height and  
427 aspect. Assuming a uniform PDFs, thirty two first order interactions with values higher than  
428 0.1% were observed for this parameter, with the most important being between Fr and Mo  
429 (5.4%) and vegetation height (4.2%), respectively, and between vegetation height and surface  
430 roughness (1.9%). Thirty one first order interactions with values higher than 0.1% were found  
431 assuming normal PDFs. The two most important are those between Fr and Mo (4.8%) and  
432 vegetation height (3.7%), respectively. Other important interactions included those between  
433 vegetation height and surface roughness (1.9%) and Mo (0.8%), respectively and between Fr and  
434 cuticle resistance (0.7%). Second or higher order interactions for this parameter assuming normal  
435 PDFs were largely similar to those observed for other parameters.

#### 436 **4.2.8 Parameter sensitivity for $\overline{NEF}_{daily}$**

437 The main and total effects for this parameter assuming both normal (Table 4, Figure 3) and  
438 uniform PDFs (Table 5) were very similar (if not identical) to those observed for  $\overline{LE}_{daily}$ . The  
439 first order interactions with values higher than 0.1% B for this parameter were very similar to  
440 those for  $\overline{EF}_{daily}$  with respect to the nature and ranking of the most important interactions  
441 assuming both normal and uniform PDFs, as were the contributions of second order or higher  
442 interactions.

443

## 444 **5 Discussion**

445 The aim of this study was to undertake a SA on the SimSphere SVAT model using **different**  
446 **atmospheric sounding data from another location** compared to previous SA studies on the model,  
447 in order to identify whether this had any impact on the model sensitivity to a set of input  
448 parameters. The most important implication of this study is that the same input parameters (in  
449 broadly the same ranking of importance) have been identified as the most significant influences  
450 on model outputs despite the SA using sounding data from a different site, in a different region

451 and under a different climatic regime. The fact that this has not shown any major differences in  
452 the nature of the model sensitivity, especially the ranking of importance is a significant step  
453 forward in terms of the model use, in that it demonstrates the applicability of the model at  
454 different sites. It has also shown that although the complex combinations of slope, aspect,  
455 vegetation and soil characteristics that are unique to each site will introduce some site-specific  
456 results (Ellis and Pomeroy, 1975), in broad terms, the most important parameters governing the  
457 sensitivity of model outputs do not change. This further confirms the findings of Petropoulos et  
458 al. (2013b,c) that by fixing the relatively unimportant model inputs to typical value ranges, the  
459 dimensionality of SimSphere could be reduced and its robustness could thus be further  
460 improved. The fact that a large number of significant first order interactions have been found for  
461 almost all the model outputs, as well as substantial contributions of higher order interactions is  
462 important since it further confirms that the model is coherent. This also suggests that no parts of  
463 the model are redundant and that there is no need to remove any element of the model  
464 architecture.

465 In common with the other recent SA experiments undertaken on SimSphere (e.g. Petropoulos et  
466 al., 2009c; 2013a-c), this article has shown that slope and aspect are the two most significant  
467 input parameters in terms of their influence on the model outputs, even assuming different PDFs.  
468 As has been outlined in these previous works, the influence of these topographic parameters is a  
469 result of their control on the amount of incoming solar radiation reaching the surface of the earth  
470 (Oliphant et al., 2003; Sabetraftar et al., 2011). As a result they will also influence LE and H  
471 fluxes surface temperature by providing energy for evapotranspiration and heat transfer through  
472 the surface energy budget. High levels of incoming solar radiation can be translated into high  
473 sensible heat transfers and into high surface temperatures. First order interactions between slope  
474 and aspect that were higher than all other first order interactions for numerous model outputs  
475 further demonstrate the sensitivity of the model outputs to these parameters.

476 Once again, in common with other SA undertaken on the model, vegetation parameters have  
477 been shown to be important, and the reasons for this have been analysed/discussed previously by  
478 Petropoulos et al., (2009c; 2013b,c). In summary, both Fr and vegetation height may influence  
479 the surface energy budget by influencing the proportion of incoming solar radiation that reaches  
480 the surface of the earth. Large Fr shade the Earth surface, and as such will influence surface  
481 temperatures. The proportion of vegetation can affect the fluxes of both LE and H fluxes through  
482 its influence on evapotranspiration, for example, as well as the proportion of incoming solar



483 radiation which is reflected and emitted by the surface. By reducing wind speed and evaporation  
484 and increasing plant transpiration, vegetation height and surface roughness can influence surface  
485 temperatures as well as the proportion of incoming solar radiation that is converted into latent or  
486 sensible heat. The influence of Mo on  $\overline{LE_{daily}}$  is to be expected, as is its influence on LE fluxes.  
487 Previous SA works on SimSphere have shown that Mo can influence air temperature (Carlson  
488 and Boland, 1978; Petropoulos et al., 2009c, Petropoulos et al., 2013c) because it can exert a  
489 significant control on evapotranspiration (Santanello et al., 2009; Dirmeyer, 2011; Lockart et al.,  
490 2012) and, therefore the partitioning of net radiation into LE and H fluxes. The importance of Fr  
491 is important since it is one of the two parameters in the “triangle” method (Gillies et al., 1997)  
492 and its more recent modifications (Chauhan et al., 2003) for deriving LE and H fluxes as well as  
493 SMC from EO data (Petropoulos et al., 2009c) and this work has shown once again that this  
494 method correctly identifies Fr and Mo as an important variables.

495 The results of this study have significant implications for the development of successful  
496 modelling approaches involving the use of SimSphere either as a standalone application or  
497 synergistically with EO data. These results evidently further confirm the model coherence and  
498 solid structure in estimating land surface interactions, supporting on-going work with the model  
499 on a global scale. Results obtained herein can be used practically to assist in future model  
500 parameterisation and implementation in diverse ecosystem conditions allowing better  
501 understanding of Earth system and feedback processes. In particular the synergistic use of  
502 SimSphere with EO data via the “triangle” method implementation appears to be a promising  
503 direction in this respect in providing regional estimates of key parameters characterising land  
504 surface interactions at different observational scales exploiting EO technology.

505

## 506 **6 Conclusions**

507 This study represents a significant step forward in the validation of the coherence of the  
508 SimSphere SVAT model, an effort currently on-going globally. Whereas previous work has  
509 examined the influence of different parameters and PDFs against real observations collected in  
510 Italy, this study examines the sensitivity of the model against data collected from a different  
511 region with a different climatic regime. In common with previous works, results confirmed that  
512 once again, model outputs are only significantly sensitive to a small group of model inputs.  
513 Slope and aspect were the most important, but the influence of vegetation parameters (vegetation  
514 height, Fr and surface roughness) and soil moisture content are also important influences on a

515 number of output parameters. Significant interactions have also been found to exist between the  
516 input parameters.. The latter suggests that the model is a coherent representation of real-world  
517 processes and in that natural feedbacks and interactions between, for example vegetation and soil  
518 moisture, are being represented.

519 In common with previous SA on SimSphere, this study has examined runs of the model at 11am.  
520 Examining the sensitivity of the model outputs at different times would be a very important  
521 direction in which future studies on SimSphere SA can be conducted. In combination with direct  
522 comparisons of the model outputs against *in-situ* “reference” estimates diurnally, conducted at  
523 different ecosystem and environmental conditions, this can assist to further extend our  
524 understanding of the SimSphere structure and establish further its coherence and correspondence  
525 to the behaviour of natural systems. It will also provide information that will be of key scientific  
526 and practical value as regards the model use, particularly as the use of SimSphere is at present  
527 expanding around the globe.

528

## 529 **Acknowledgments**

530 Dr. Petropoulos gratefully acknowledges the financial support provided by the European  
531 Commission under the Marie Curie Career Re-Integration Grant “TRANSFORM-EO” project  
532 for the completion of this work.

533

## 534 **References**

535 Battrick, B. The Changing Earth. New Scientific Challenges for ESA’s Living Planet  
536 Programme. ESA SP-1304. ESA Publications Division, ESTEC, The Netherlands, 2006.

537 Carlson, T.N. An overview of the “triangle method” for estimating surface evapotranspiration  
538 and soil moisture from satellite imagery. *Sensors*, 7, 1612–1629, 2007.

539 Carlson, T.N. and Boland, F.E. Analysis of urban-rural canopy using a surface heat  
540 flux/temperature model. *Journal of Applied Meteorology*, 17, 998–1014, 1978, 1978.

541 Carlson, T.N., Dodd, J.K., Benjamin, S.G. and Cooper, J.N. Satellite estimation of the surface  
542 energy balance, moisture availability and thermal inertia. *Journal of Applied Meteorology*, 20,  
543 67-87, 1981.

544 Chauhan, N.S., Miller, S. and Ardanuy, P. Spaceborne soil moisture estimation at high  
545 resolution: amicrowave-optical/IR synergistic approach. *International Journal of Remote*  
546 *Sensing*, 22, 4599–4646, 2003.

547 Chen, L., Tian, Y., Cao, C., Zhang, S. and Zhang, S. Sensitivity and uncertainty analysis of an  
548 extended ASM3-SMP model describing membrane bioreactor operation. *Journal of Membrane*  
549 *Science*, 389, 99-109, 2012.

550 Dirmeyer, P.A. The terrestrial segment of soil moisture-climate coupling. *Geophysical Research*  
551 *Letters*, 38, L16702, 2011.

552 Ellis, C.R. and Pomeroy, J.W. Estimating sub-canopy shortwave irradiance to melting snow on  
553 forested slopes. *Hydrological Processes*, 21, 2581-2593, 1975.

554 European Space Agency, Support to Science Element 2012 A pathfinder for innovation in Earth  
555 Observation, pp. 41, ESA, 2012. Available from:  
556 [http://due.esrin.esa.int/stse/files/document/STSE\\_report\\_121016.pdf](http://due.esrin.esa.int/stse/files/document/STSE_report_121016.pdf) [accessed on 10/07/2013].

557 Gillies, R.R. and Carlson, T.N. Thermal remote sensing of surface soil moisture content with  
558 partial vegetation cover for incorporation into climate models. *Journal of Applied Meteorology*,  
559 34, 745-756, 1995.

560 Gillies, R.R., Carlson, T.N., Cui, J., Kustas, W.P. and Humes, K.S. Verification of the “triangle”  
561 method for obtaining surface soil moisture content and energy fluxes from remote measurements  
562 of the Normalised Difference Vegetation Index (NDVI) and surface radiant temperatures.  
563 *International Journal of Remote Sensing*, 18, 3145-3166, 1997.

564 Holvoet, K., van Griensven, A., Seuntjents, P. and Vanrolleghem, P.A. Sensitivity analysis for  
565 hydrology and pesticide supple towards the river in SVAT. *Physics and Chemistry of the Earth*,  
566 30, 518-526, 2005.

567 Johnson, J.S., Gosling, J.P. and Kennedy, M.C. Gaussian process emulation for second-order  
568 Monte Carlo simulations. *Journal of Statistical Planning and Inference*, 141, 1838-1848, 2011.

569 Kennedy, M. C., Butler Ellis, M. C. and Miller, P.C.H. BREAM: A probabilistic Bystander and  
570 Resident Exposure Assessment Model of spray drift from an agricultural boom sprayer.  
571 *Computers and Electronics in Agriculture*, 88, 63-71, 2012.

572 Kennedy, M.C. Description of the Gaussian processes model used in GEM-SA, GEM-SA Help  
573 Documentation, 2004.

574 Kennedy, M.C. and O'Hagan, A. Bayesian calibration of computer models. *Journal of the Royal*  
575 *Statistical Society Series B*, 63, 425–464, 2011.

576 Kimeldorf, G. and Wahba, G. Some results on Tchebycheffian spline functions. *Journal of*  
577 *Mathematical Analysis and Applications*, 33, 82-95, 1971.

578 Kustas, W. and Anderson, M. Advances in thermal infrared remote sensing for land surface  
579 modelling. *Agricultural and Forest Meteorology*, 149, 2071-2081, 2009.

580 Lockart, N., Kavetski, D. and Franks, S.W. On the role of soil moisture in daytime evolution of  
581 temperatures. *Hydrological Processes* DOI:10.1002/hyp.9525, 2012.

582 Nossent, J., Elsen, P. and Bauwens, W. Sobol's sensitivity analysis of a complex environmental  
583 model. *Environmental Modelling and Software*, 26, 1515-1525, 2011.

584 O'Hagan, A. Curve fitting and optimal design for prediction (with discussion). *Journal of the*  
585 *Royal Statistical Society Series B*, 40, 1-42, 1978.

586 Oakley, J. and O'Hagan, A. Probabilistic sensitivity analysis of complex models: A Bayesian  
587 approach. *Journal of the Royal Statistical Society Series B*, 66, 751-769, 2004.

588 Oliosio, A. Simulation des échanges d'énergie et de masse d'un couvert végétal, dans le but de  
589 relier la transpiration et la photosynthèse aux mesures de réflectance et de température de  
590 surface. PhD Thesis, University de Montpellier II, 1992.

591 Oliosio, A., Chauki, H., Courault, D. and Wigneron, J.-P. Estimation of evapotranspiration and  
592 photosynthesis by assimilation of remote sensing data into SVAT models. *Remote Sensing of*  
593 *Environment*, 68, 341–356, 1999.

594 Oliphant, A.J., Spronken-Smith, R.A., Sturman, A.P. and Owens, I.F. Spatial variability of  
595 surface radiation fluxes in mountainous terrain. *Journal of Applied Meteorology*, 42, 113-128,  
596 2003.

597 Parry, H.R., Topping, C.J., Kennedy, M.C., Boatman, N.D. and Murray, A.W.A. Bayesian  
598 sensitivity analysis applied to an Agent-based model of bird population response to landscape  
599 change. *Environmental Modelling and Software*, 45, 1-12, 2012.

600 **Petropoulos G. and Carlson, T.N. Retrievals of turbulent heat fluxes and soil moisture content by**  
601 **Remote Sensing, p. 667-502, in Advances in Environmental Remote Sensing: Sensors,**  
602 **Algorithms, and Applications, Ed. Taylor and Francis, 556, 2011.**

603 Petropoulos G.P. Remote Sensing of Surface Turbulent Energy Fluxes. Chapter 3, pp: 53-88. In  
604 Remote Sensing of Energy Fluxes and Soil Moisture Content, Petropoulos, G.P (ed) Taylor and  
605 Francis, [in press], 2013.

606 Petropoulos, G.P., Konstas, I., and Carlson, T.N. Automation of SimSphere Land Surface Model  
607 Use as a Standalone Application and Integration with EO Data for Deriving Key Land Surface  
608 Parameters. European Geosciences Union, April 7-12<sup>th</sup>, 2013, Vienna, Austria, 2013a.

609 Petropoulos, G., Carlson, T.N. and Wooster, M. J. An Overview of the Use of the SimSphere  
610 Soil Vegetation Atmosphere Transfer (SVAT) Model for the Study of Land-Atmosphere  
611 Interactions. *Sensors*, 9(6), 4286-4308, 2009a.

612 Petropoulos, G., Carlson, T.N, Wooster, M. J. and Islam, S. A Review of Ts/VI Remote Sensing  
613 Based Methods for the Retrieval of Land Surface Fluxes and Soil Surface Moisture Content.  
614 *Advances in Physical Geography*, 33 (2), 1-27. 2009b.

615 Petropoulos, G., Wooster, M. J., Kennedy, M., Carlson, T.N. and Scholze, M. A global  
616 sensitivity analysis study of the 1d SimSphere SVAT model using the GEM SA software.  
617 *Ecological Modelling*, 220 (19), 2427-2440, 2009c.

618 Petropoulos, G., Ratto, M. and Tarantola, S. A comparative analysis of emulators for the  
619 sensitivity analysis of a land surface process model. 6<sup>th</sup> International Conference on Sensitivity  
620 Analysis of Model Output, July 19-22<sup>nd</sup>, 2010, Milan, Italy, on *Procedia - Social and Behavioral*  
621 *Sciences*, vol. 2 (6), 7716-17, 2010.

622 Petropoulos, G.P., Griffiths, H.M. and Tarantola, S. Towards Operational Products Development  
623 from Earth Observation: Exploration of SimSphere Land Surface Process Model Sensitivity  
624 using a GSA approach. 7th International Conference on Sensitivity Analysis of Model Output,  
625 July 1-4th, 2013, Nice, France, 2013a.

626 Petropoulos G., Griffiths, H.M. and Ioannou-Katidis, P. Sensitivity Exploration of SimSphere  
627 Land Surface Model Towards its Use for Operational Products Development from Earth  
628 Observation Data, Chapter 14, 21 pages. To appear in book titled as “Advancement in Remote  
629 Sensing for Environmental Applications”, edited by S. Mukherjee, M. Gupta, P.K. Srivastava  
630 and T. Islam, Springer [in press], 2013b.

631 Petropoulos, G.P., H. Griffiths and S. Tarantola. Sensitivity Analysis of the SimSphere SVAT  
632 Model in the Context of EO-based Operational Products Development. *Environmental*  
633 *Modelling and Software* [accepted], 2013c.

634 Piles, M. Camps, A., Vall-llossera, M., Corbella, I., Panciera, R., Rudiger, C., Kerr, Y.H. and  
635 Walker, J. Downscaling SMOS-Derived Soil Moisture Using MODIS Visible/Infrared Data.  
636 *IEEE Transactions on Geosciences and Remote Sensing*, 49(9), 3156 – 3166, 2011.

637 Ratto, M., Tarantola, S. and Saltelli, A. Sensitivity analysis in model calibration: GSA-GLUE  
638 approach. *Computer Physics Communications*, 136, 212-224, 2011.

639 Sabetraftar, K., Mackey, B. and Croke, B. Sensitivity of modelling gross primary productivity to  
640 topographic effects on surface radiation: A case study in the Cotter River Catchment, Australia.  
641 *Ecological Modelling*, 222, 795-803, 2011.

642 Saltelli, A., Chan, K. and Scott, E.M. Sensitivity analysis. In: *Wiley Series in Probability and*  
643 *Statistics*. 467 Wiley, Chichester, 2000.

644 Saltelli, A., Tarantola, S. and Chan, K.P.-S. A quantitative model-independent method for global  
645 sensitivity analysis of model output. *Technometrics*, 41 (1), 39–56, 1999.

646 Santanello, J.A., Peters-Lidard, C.D., Kumar, S.V., Alonge, C. and Tao, W.-K. A modelling and  
647 observational framework for diagnosing local land-atmosphere coupling on diurnal timescales.  
648 *Journal of Hydrometeorology*, 10, 577-599, 2009.

649 Seneviratne, S.I., Corti, T., Davin, E. L. Hirschi, M. Jaeger, E.B. Lehner, I. Orlowsky, B. and  
650 Teuling, A.J. Investigating soil moisture–climate interactions in a changing climate: A review.  
651 *Earth Sciences Reviews* 99 (3-4):125-161, 2010.

652 Song, X., Bryan, B.A., Paul, K.I., Zhao, G. Variance-based sensitivity analysis of a forest  
653 growth model, *Ecological Modelling*, 246, 135-143, 2012.

Table 1. Summary of the SimSphere inputs considered in the GSA implementation. Units of each of the model inputs, where appropriate, are provided in brackets.

Model input short name	Actual name of the model input	Process in which each parameter is involved	Min value	Max value
X1	Slope ( <i>degrees</i> )	time & location	0	45
X2	Aspect ( <i>degrees</i> )	time & location	0	360
X3	Station Height ( <i>meters</i> )	time & location	0	4.92
X4	Fractional Vegetation Cover (%)	vegetation	0	100
X5	LAI ( <i>m<sup>2</sup>m<sup>-2</sup></i> )	vegetation	0	10
X6	Foliage emissivity ( <i>unitless</i> )	vegetation	0.951	0.990
X7	[Ca] (external [CO <sub>2</sub> ] in the leaf) ( <i>ppmv</i> )	vegetation	250	710
X8	[Ci] (internal [CO <sub>2</sub> ] in the leaf) ( <i>ppmv</i> )	vegetation	110	400
X9	[O3] (ozone concentration in the air) ( <i>ppmv</i> )	vegetation	0.0	0.25
X10	Vegetation height ( <i>meters</i> )	vegetation	0.021	20.0
X11	Leaf width ( <i>meters</i> )	vegetation	0.012	1.0
X12	Minimum Stomatal Resistance ( <i>sm<sup>-1</sup></i> )	plant	10	500
X13	Cuticle Resistance ( <i>sm<sup>-1</sup></i> )	plant	200	2000
X14	Critical leaf water potential ( <i>bar</i> )	plant	-30	-5
X15	Critical solar parameter ( <i>Wm<sup>-2</sup></i> )	plant	25	300
X16	Stem resistance ( <i>sm<sup>-1</sup></i> )	plant	0.011	0.150
X17	Surface Moisture Availability ( <i>vol/vol</i> )	hydrological	0	1
X18	Root Zone Moisture Availability ( <i>vol/vol</i> )	hydrological	0	1
X19	Substrate Max. Volum. Water Content ( <i>vol/vol</i> )	hydrological	0.01	1
X20	Substrate climatol. mean temperature ( <i>°C</i> )	surface	20	30
X21	Thermal inertia ( <i>Wm<sup>-2</sup>K<sup>-1</sup></i> )	surface	3.5	30
X22	Ground emissivity ( <i>unitless</i> )	surface	0.951	0.980
X23	Atmospheric Precipitable water ( <i>cm</i> )	meteorological	0.05	5
X24	Surface roughness ( <i>meters</i> )	meteorological	0.02	2.0
X25	Obstacle height ( <i>meters</i> )	meteorological	0.02	2.0
X26	Fractional Cloud Cover (%)	meteorological	1	10
X27	RKS (satur. thermal conduct.)( <i>Cosby et al., 1984</i> )	soil	0	10
X28	Cosby B (see <i>Cosby et al., 1984</i> )	soil	2.0	12.0
X29	THM (satur.vol. water cont.)( <i>Cosby et al., 1984</i> )	soil	0.3	0.5
X30	PSI (satur. water potential) ( <i>Cosby et al., 1984</i> )	soil	1	7

Table 2. Emulator accuracy statistics for the SA tests conducted in our study (under both normal and uniform PDFs assumptions for the model inputs/outputs).

<b>Fitted model parameters (based on standardised input/output)</b>	$\overline{Rn}_{daily}$	$\overline{H}_{daily}$	$\overline{LE}_{daily}$	$\overline{Trad}_{daily}$	$\overline{Mo}_{daily}$	$\overline{Tair}_{daily}$	$\overline{EF}_{daily}$	$\overline{NEF}_{daily}$
<b>Sigma-squared:</b>	0.413	1.619	1.057	0.875	1.240	1.630	1.483	1.483
<b>Emulator accuracy:</b>								
<b>Cross-validation root mean squared-error (wm-2):</b>	25.060	34.776	28.798	2.771	31.012	0.491	0.082	0.082
<b>Cross-validation root mean squared relative error (%):</b>	6.349	41.633	23.485	7.913	13.814	3.030	20.033	25.292
<b>Cross-validation root mean squared standardised error:</b>	1.111	1.790	1.484	1.117	1.474	1.505	1.717	1.717



Table 3. Summarised statistics concerning the emulator accuracy evaluation for the different SimSphere model outputs examined in our study. Shading highlights the roughness values of the model inputs with values greater than 1.0. Rows X1 to X30 show roughness values for the different model outputs examined (for normal and uniform PDFs).

<b>Model Inputs</b>	$\overline{Rn}_{daily}$	$\overline{H}_{daily}$	$\overline{LE}_{daily}$	$\overline{Trad}_{daily}$	$\overline{Mo}_{daily}$	$\overline{Tair}_{daily}$	$\overline{EF}_{daily}$	$\overline{NEF}_{daily}$
<b>X1</b>	1.842	0.092	0.479	0.755	0.688	0.488	0.049	0.049
<b>X2</b>	12.728	4.317	8.451	8.557	7.638	7.247	0.617	0.617
<b>X3</b>	0.156	0.289	0.105	0.013	0.611	0.187	0.043	0.043
<b>X4</b>	0.643	0.672	0.931	1.307	0.668	0.838	1.845	1.845
<b>X5</b>	0.608	0.065	0.062	0.223	1.027	0.035	0.150	0.150
<b>X6</b>	0.022	0.053	0.000	0.015	0.010	0.000	0.000	0.000
<b>X7</b>	0.001	0.102	0.094	0.000	0.012	0.000	0.091	0.091
<b>X8</b>	0.000	0.007	0.016	0.000	0.038	0.005	0.035	0.035
<b>X9</b>	0.174	0.172	0.121	0.338	0.018	0.201	0.002	0.002
<b>X10</b>	0.377	2.389	0.000	1.036	0.137	2.272	4.396	4.396
<b>X11</b>	0.019	0.054	0.040	0.034	0.156	0.030	0.030	0.030
<b>X12</b>	0.000	0.008	0.003	0.000	0.000	0.000	0.386	0.386
<b>X13</b>	0.022	0.048	0.161	0.043	0.030	0.040	0.217	0.217
<b>X14</b>	0.014	0.000	0.001	0.010	0.004	0.019	0.037	0.037
<b>X15</b>	0.016	0.000	0.000	0.071	0.000	0.009	0.000	0.000
<b>X16</b>	0.011	0.023	0.048	0.058	0.047	0.000	0.033	0.033
<b>X17</b>	1.197	2.146	1.416	1.048	0.408	0.422	1.346	1.346
<b>X18</b>	0.025	0.000	0.056	0.007	0.131	0.000	0.135	0.135
<b>X19</b>	0.000	0.000	0.077	0.004	0.048	0.000	0.070	0.070
<b>X20</b>	0.012	0.006	0.054	0.000	0.107	0.005	0.000	0.000
<b>X21</b>	0.005	0.013	0.000	0.000	0.000	0.002	0.011	0.011
<b>X22</b>	0.007	0.000	0.101	0.041	0.000	0.000	0.010	0.010
<b>X23</b>	0.004	0.000	0.042	0.104	0.055	0.003	0.098	0.098
<b>X24</b>	0.176	3.328	0.064	0.185	0.329	4.195	1.384	1.384
<b>X25</b>	0.030	0.000	0.053	0.145	0.169	0.070	0.000	0.000
<b>X26</b>	0.008	0.089	0.058	0.032	0.000	0.000	0.105	0.105
<b>X27</b>	0.000	0.000	0.092	0.000	0.026	0.000	0.000	0.000

<b>X28</b>	0.012	0.046	0.125	0.034	0.222	0.000	0.091	0.091
<b>X29</b>	0.079	0.178	0.092	0.102	0.204	0.026	0.022	0.022
<b>X30</b>	0.079	0.006	1.710	0.083	0.054	0.174	0.003	0.003

Table 4. Summarised results from the implementation of the BACCO GEM SA method on the different outputs simulated by SimSphere using the normal PDFs. Computed main (ME) and total effect (TE) indices by the GEM tool (expressed as %) for each of the model parameters are shown whereas the last three lines summarise the percentages of the explained total output variance of the main effects alone and after including the interaction effects. Input parameters with a variance decomposition of greater than 1 % are highlighted in grey.

Model Input	$Rn_{daily}$		$H_{daily}$		$LE_{daily}$		$Trad_{daily}$		$Mo_{daily}$		$Tair_{daily}$		$EF_{daily}$		$NEF_{daily}$	
	ME	TE	ME	TE	ME	TE	ME	TE	ME	TE	ME	TE	ME	TE	ME	TE
X1	20.294	31.964	1.388	3.078	7.969	16.245	12.676	24.032	17.129	29.450	1.846	10.150	0.991	1.613	0.991	1.613
X2	50.095	63.626	10.944	31.147	36.024	51.870	34.857	52.048	28.462	50.207	21.877	43.797	4.283	8.883	4.283	8.882
X3	0.016	0.353	0.469	4.245	0.066	0.825	0.031	0.150	1.278	4.853	0.411	2.482	0.130	0.610	0.130	0.610
X4	7.161	8.916	15.239	25.509	8.132	16.975	5.586	10.606	0.704	6.702	16.655	25.647	10.362	26.932	10.362	26.932
X5	2.060	3.357	0.135	1.710	0.184	0.709	0.049	1.462	12.028	20.080	0.071	0.672	0.060	1.824	0.060	1.824
X6	0.014	0.094	0.142	1.136	0.027	0.028	0.048	0.177	0.030	0.151	0.020	0.022	0.032	0.034	0.032	0.034
X7	0.010	0.015	0.090	2.166	0.049	0.855	0.028	0.029	0.054	0.198	0.037	0.039	0.065	1.086	0.065	1.086
X8	0.008	0.008	0.120	0.262	0.031	0.181	0.020	0.021	0.065	0.474	0.102	0.200	0.060	0.544	0.060	0.544
X9	0.029	0.465	0.093	3.309	0.098	0.898	0.149	1.703	0.032	0.222	0.067	2.669	0.093	0.120	0.093	0.120
X10	0.427	1.234	10.357	29.664	0.015	0.016	3.293	7.415	0.803	2.066	7.832	22.447	8.155	24.214	8.155	24.214
X11	0.021	0.095	0.275	1.401	0.350	0.677	0.127	0.432	0.177	2.093	0.044	0.500	0.308	0.759	0.308	0.759
X12	0.006	0.007	0.137	0.306	0.065	0.091	0.026	0.027	0.033	0.034	0.058	0.060	0.442	3.400	0.442	3.400
X13	0.134	0.203	0.158	1.041	1.546	2.699	0.609	0.922	0.151	0.490	0.247	0.929	1.652	4.295	1.653	4.295
X14	0.013	0.066	0.088	0.090	0.037	0.052	0.074	0.155	0.131	0.174	0.097	0.395	0.155	0.599	0.155	0.599
X15	0.024	0.077	0.037	0.039	0.041	0.042	0.070	0.506	0.030	0.031	0.122	0.260	0.025	0.026	0.025	0.026
X16	0.021	0.057	0.242	0.717	0.021	0.422	0.168	0.563	0.042	0.648	0.055	0.057	0.042	0.477	0.042	0.477
X17	3.554	5.219	11.669	26.284	17.567	27.166	16.911	21.465	3.563	7.129	7.010	11.169	38.200	49.518	38.199	49.518
X18	0.071	0.160	0.099	0.101	0.251	0.707	0.095	0.159	0.054	1.229	0.143	0.145	0.835	2.507	0.835	2.507
X19	0.010	0.010	0.054	0.056	0.643	1.300	0.056	0.090	0.284	0.735	0.033	0.035	0.286	1.055	0.286	1.056
X20	0.083	0.125	0.190	0.308	0.098	0.538	0.346	0.347	0.749	1.608	0.167	0.256	0.036	0.038	0.036	0.038
X21	0.032	0.050	0.228	0.487	0.029	0.030	0.043	0.044	0.035	0.037	0.105	0.137	0.072	0.234	0.072	0.234
X22	0.016	0.043	0.119	0.121	0.130	0.841	0.043	0.449	0.055	0.057	0.094	0.096	0.045	0.194	0.045	0.194
X23	0.009	0.025	0.052	0.054	0.032	0.378	0.042	0.718	0.124	0.653	0.025	0.081	0.066	1.239	0.066	1.239
X24	0.285	0.745	3.509	24.425	0.222	0.707	0.853	2.332	1.391	4.019	6.465	23.644	1.318	9.913	1.318	9.913
X25	0.010	0.129	0.049	0.051	0.044	0.552	0.051	1.067	0.061	1.551	0.042	1.070	0.075	0.076	0.075	0.076
X26	0.030	0.059	0.264	2.020	0.079	0.625	0.087	0.368	0.051	0.052	0.047	0.049	0.050	1.240	0.050	1.240
X27	0.005	0.005	0.043	0.045	0.032	0.909	0.017	0.018	0.053	0.330	0.031	0.033	0.026	0.028	0.026	0.028

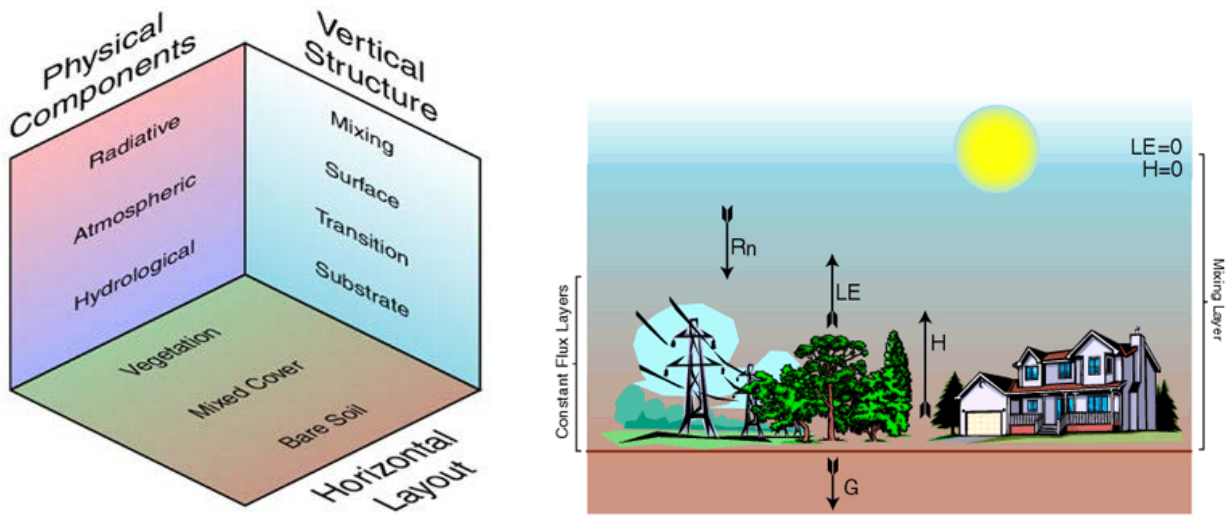
<b>X28</b>	0.035	0.075	0.072	1.019	0.044	0.882	0.049	0.321	0.374	2.540	0.082	0.084	0.224	1.261	0.224	1.261
<b>X29</b>	0.058	0.289	0.402	2.995	0.028	0.866	0.344	1.024	0.103	2.105	0.206	0.585	0.118	0.404	0.118	0.404
<b>X30</b>	0.036	0.276	0.074	0.199	0.285	5.121	0.096	0.781	0.042	0.661	0.071	2.333	0.052	0.099	0.052	0.099
<b>Main effects Only</b>	<b>84.568</b>		<b>56.735</b>		<b>74.138</b>		<b>76.844</b>		<b>68.091</b>		<b>64.061</b>		<b>68.258</b>		<b>68.258</b>	
<b>1<sup>st</sup> Order Interactions Only</b>	<b>13.486</b>		<b>26.454</b>		<b>19.706</b>		<b>17.916</b>		<b>24.610</b>		<b>24.309</b>		<b>22.129</b>		<b>22.129</b>	
<b>2<sup>nd</sup> or Higher Order Interactions</b>	<b>1.946</b>		<b>16.810</b>		<b>6.155</b>		<b>5.240</b>		<b>7.299</b>		<b>11.630</b>		<b>9.613</b>		<b>9.613</b>	

Table 5. Summarised results from the implementation of the BACCO GEM SA method on the different outputs simulated by SimSphere using the uniform PDFs. Computed main (ME) and total effect (TE) indices by the GEM tool (expressed as %) for each of the model parameters are shown whereas the last three lines summarise the percentages of the explained total output variance of the main effects alone and after including the interaction effects. Input parameters with a variance decomposition of greater than 1 % are highlighted in grey.

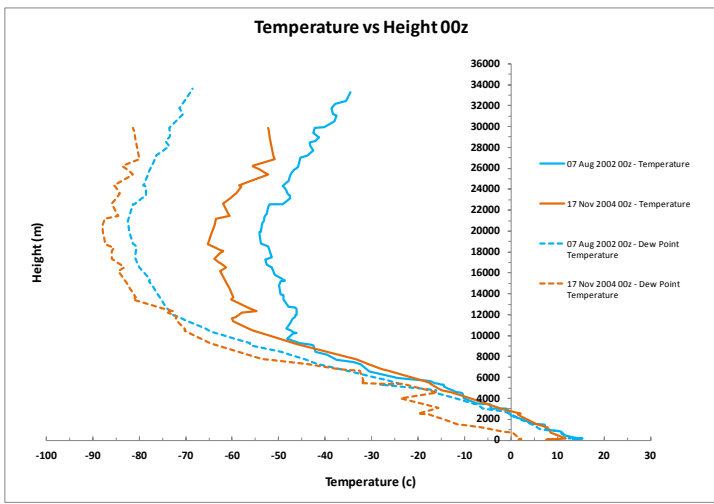
Model Input	$Rn_{daily}$		$H_{daily}$		$LE_{daily}$		$Trad_{daily}$		$Mo_{daily}$		$Tair_{daily}$		$EF_{daily}$		$NEF_{daily}$	
	ME	TE	ME	TE	ME	TE	ME	TE	ME	TE	ME	TE	ME	TE	ME	TE
<b>X1</b>																
<b>X2</b>	12.975	28.482	1.275	3.143	4.924	14.568	8.652	21.467	0.004	0.137	1.629	11.437	1.060	1.835	1.060	1.836
<b>X3</b>	48.063	65.740	8.488	30.090	29.778	48.045	29.559	49.160	0.030	0.225	18.069	43.831	2.378	7.725	2.378	7.725
<b>X4</b>	0.011	0.486	0.493	4.965	0.062	1.103	0.054	0.207	0.005	0.064	0.227	3.012	0.126	0.747	0.126	0.747
<b>X5</b>	9.495	12.012	16.600	28.455	8.924	21.070	5.572	12.051	0.069	0.106	16.940	28.347	9.465	30.328	9.465	30.328
<b>X6</b>	2.588	4.589	0.190	1.926	0.255	0.920	0.046	2.046	0.002	0.002	0.073	0.835	0.043	2.241	0.043	2.241
<b>X7</b>	0.010	0.121	0.122	1.265	0.030	0.031	0.044	0.210	0.004	0.004	0.023	0.025	0.035	0.037	0.035	0.037
<b>X8</b>	0.013	0.020	0.078	2.519	0.044	1.150	0.032	0.033	0.004	0.019	0.042	0.044	0.043	1.353	0.043	1.353
<b>X9</b>	0.010	0.010	0.096	0.253	0.042	0.234	0.023	0.025	0.006	0.093	0.098	0.218	0.045	0.653	0.045	0.653
<b>X10</b>	0.035	0.646	0.148	3.845	0.072	1.130	0.140	2.224	0.001	0.020	0.165	3.944	0.100	0.134	0.100	0.134
<b>X11</b>	0.459	1.614	8.144	30.406	0.017	0.018	2.941	8.203	0.002	0.003	5.886	23.266	7.743	27.736	7.743	27.737
<b>X12</b>	0.041	0.140	0.325	1.595	0.342	0.765	0.209	0.603	0.003	0.032	0.046	0.651	0.287	0.857	0.287	0.857
<b>X13</b>	0.008	0.008	0.150	0.341	0.072	0.104	0.030	0.031	0.003	0.003	0.065	0.068	0.341	4.153	0.341	4.153
<b>X14</b>	0.179	0.277	0.249	1.234	1.791	3.330	0.689	1.110	0.014	0.038	0.418	1.263	1.885	5.225	1.885	5.225
<b>X15</b>	0.014	0.088	0.087	0.089	0.041	0.060	0.085	0.191	0.005	0.022	0.105	0.496	0.135	0.699	0.135	0.699
<b>X16</b>	0.035	0.111	0.037	0.039	0.046	0.047	0.077	0.682	0.003	0.003	0.149	0.326	0.027	0.029	0.027	0.029
<b>X17</b>	0.026	0.076	0.280	0.811	0.023	0.536	0.172	0.699	0.002	0.002	0.062	0.065	0.060	0.620	0.060	0.620
<b>X18</b>	4.907	7.116	11.788	28.159	20.154	33.046	22.206	28.072	96.361	97.557	8.174	13.430	35.735	49.092	35.735	49.092
<b>X19</b>	0.073	0.196	0.098	0.100	0.321	0.921	0.112	0.195	0.346	0.472	0.162	0.164	0.635	2.692	0.635	2.692
<b>X20</b>	0.012	0.013	0.053	0.055	0.708	1.564	0.061	0.105	0.950	2.090	0.037	0.039	0.297	1.262	0.297	1.262
<b>X21</b>	0.092	0.151	0.188	0.319	0.117	0.693	0.396	0.398	0.001	0.002	0.181	0.294	0.039	0.041	0.039	0.041
<b>X22</b>	0.038	0.062	0.192	0.480	0.032	0.034	0.049	0.051	0.002	0.009	0.116	0.156	0.079	0.280	0.079	0.280
<b>X23</b>	0.027	0.065	0.117	0.120	0.120	1.052	0.026	0.532	0.002	0.002	0.106	0.108	0.048	0.233	0.048	0.233
<b>X24</b>	0.011	0.034	0.051	0.054	0.036	0.495	0.048	0.955	0.003	0.003	0.028	0.099	0.071	1.620	0.071	1.620
<b>X25</b>	0.405	1.081	3.761	27.617	0.281	0.913	1.136	3.181	0.006	0.015	4.772	26.161	1.217	12.448	1.217	12.448

<b>X26</b>	0.009	0.184	0.049	0.051	0.031	0.687	0.041	1.452	0.009	0.019	0.080	1.392	0.081	0.083	0.081	0.083
<b>X27</b>	0.031	0.073	0.250	2.123	0.079	0.774	0.067	0.429	0.004	0.004	0.053	0.055	0.041	1.584	0.041	1.584
<b>X28</b>	0.006	0.007	0.042	0.045	0.041	1.128	0.020	0.021	0.015	0.454	0.035	0.037	0.028	0.030	0.028	0.030
<b>X29</b>	0.049	0.106	0.082	1.130	0.040	1.145	0.091	0.446	0.058	0.797	0.093	0.095	0.373	1.682	0.372	1.682
<b>X30</b>	0.092	0.436	0.470	3.459	0.090	1.130	0.488	1.384	0.010	0.417	0.201	0.687	0.115	0.480	0.115	0.480
	0.022	0.361	0.082	0.220	0.137	6.415	0.046	0.956	0.026	1.103	0.060	3.286	0.055	0.113	0.055	0.113
<b>Main effects Only</b>	79.736		53.985		68.651		73.112		97.950		58.096		62.586		62.586	
<b>1<sup>st</sup> Order Interactions Only</b>	17.077		24.146		22.103		18.889		0.830		24.932		22.731		22.731	
<b>2<sup>nd</sup> or Higher Order Interactions</b>	3.187		21.869		9.246		7.999		1.220		16.972		14.683		14.683	

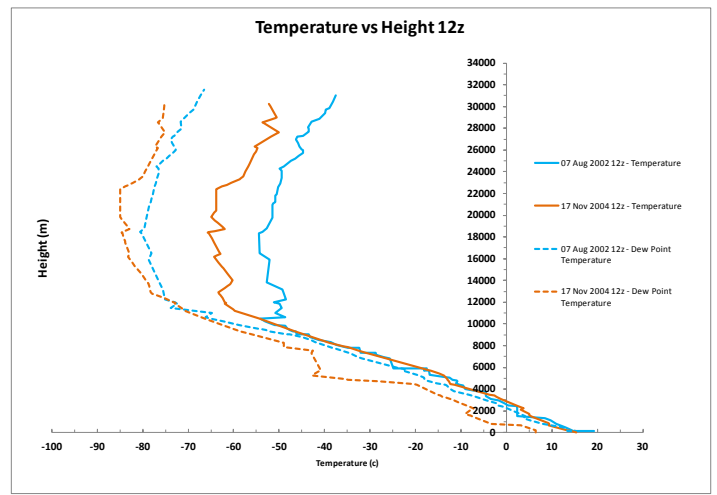
0 List of Figures:



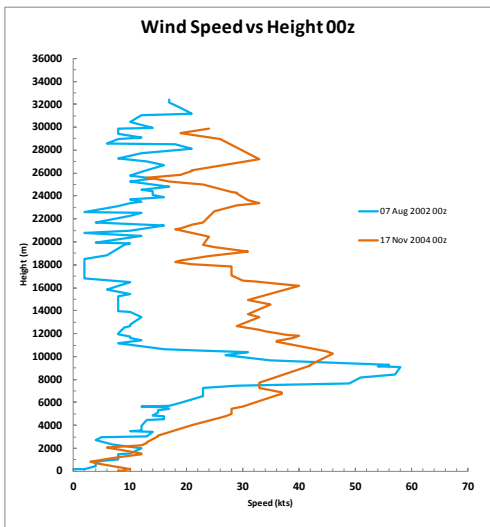
4 **Figure 1.** Left: The different layers of the SVAT model in the vertical domain; Right: a schematic  
5 representation of the surface energy balance components computation in the SVAT model (after SimSphere  
6 User's manual available at [http://www.aber.ac.uk/en/iges/research-groups/earth-observation-](http://www.aber.ac.uk/en/iges/research-groups/earth-observation-laboratory/simsphere/workbook/preface/)  
7 [laboratory/simsphere/workbook/preface/](http://www.aber.ac.uk/en/iges/research-groups/earth-observation-laboratory/simsphere/workbook/preface/)).



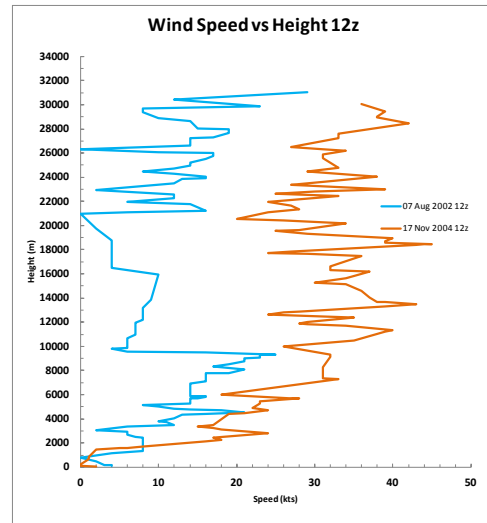
(a).



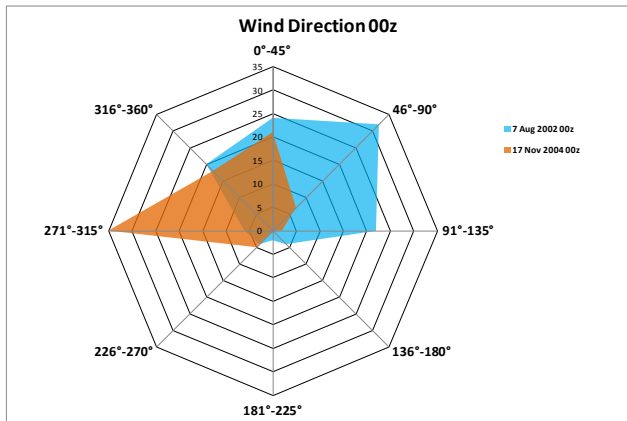
(b).



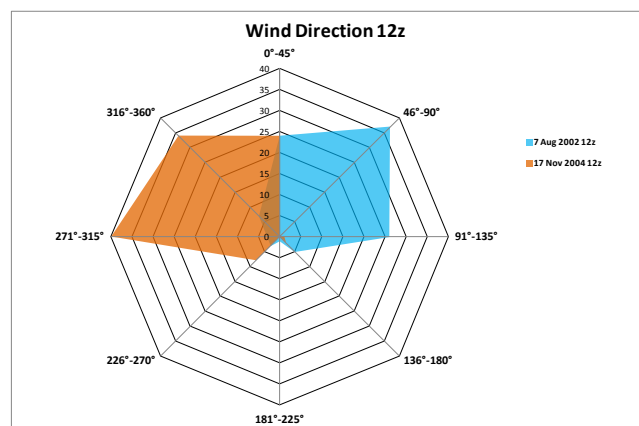
(c).



(d).



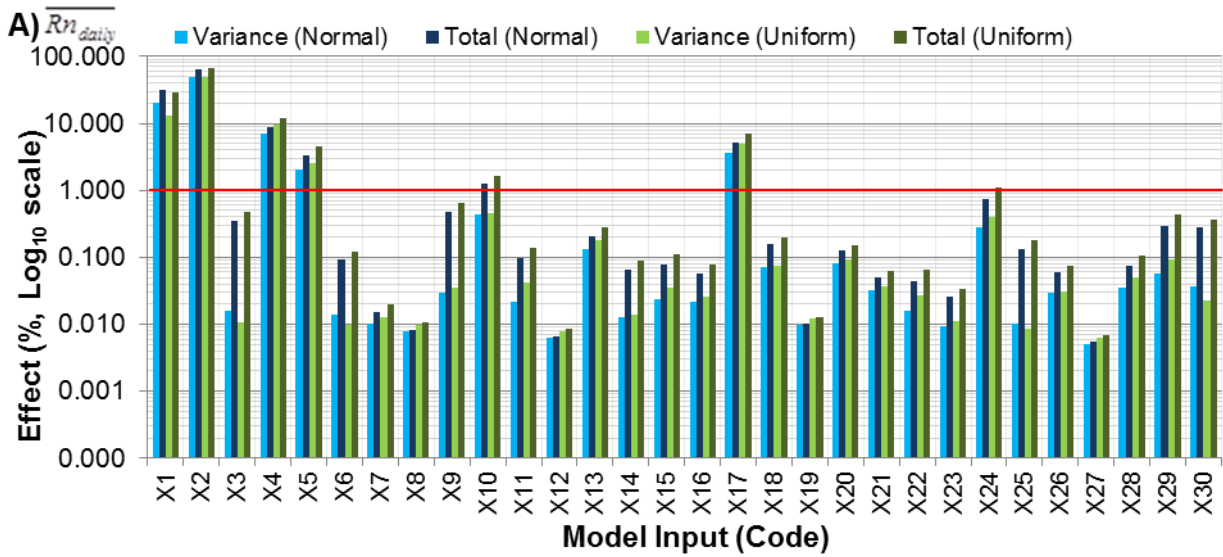
(e).



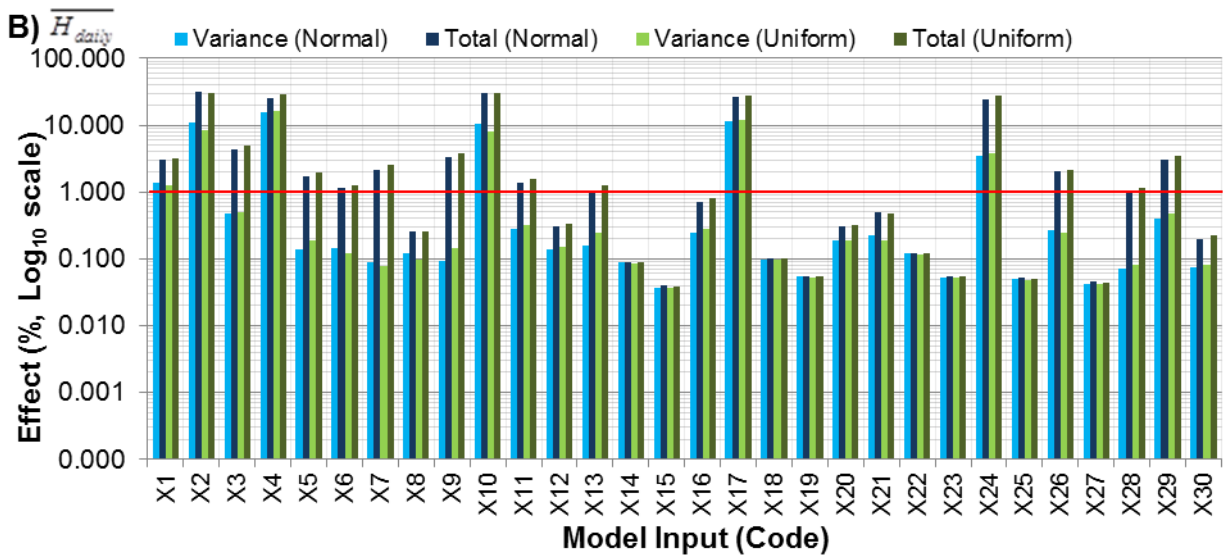
(f).

**Figure 2:** Atmospheric soundings used in the present study in comparison to the Petropoulos et al., (2009d) Study for temperature (a,b), wind direction (c-d) and wind speed (e,f).

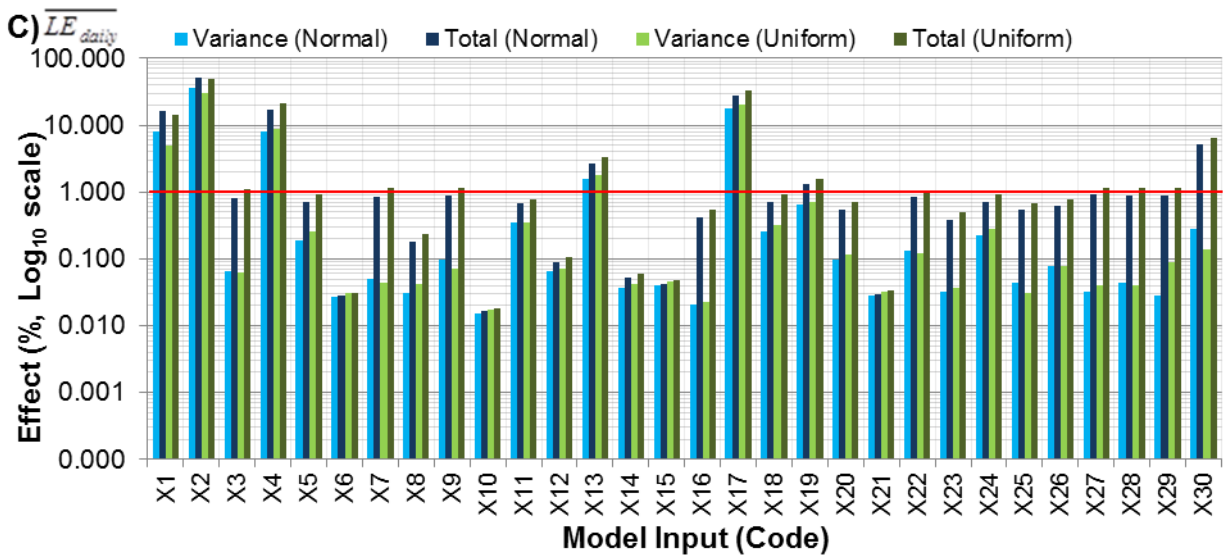




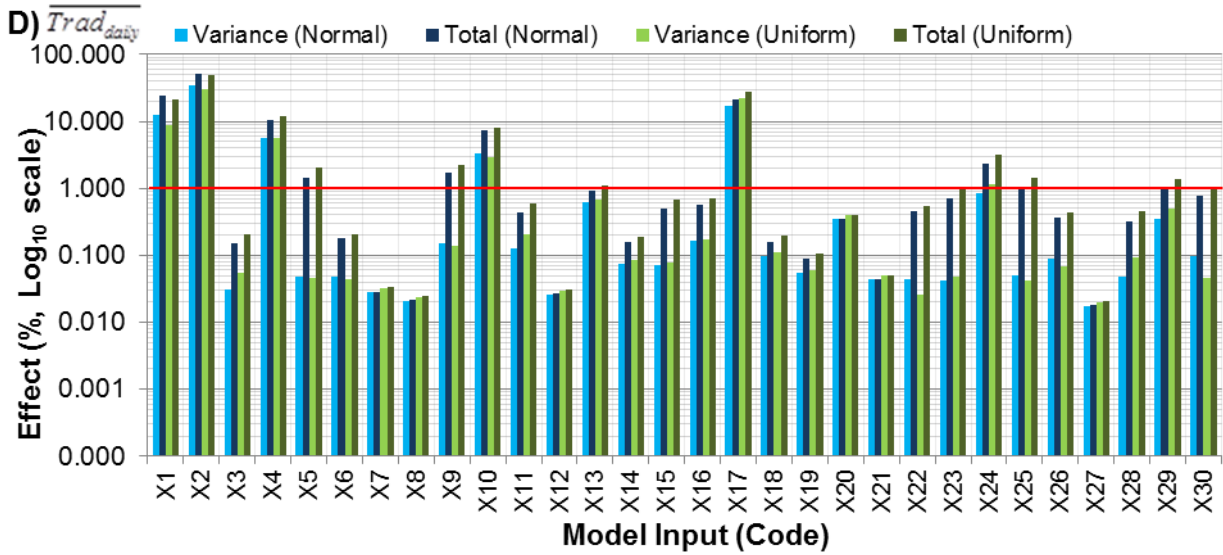
20



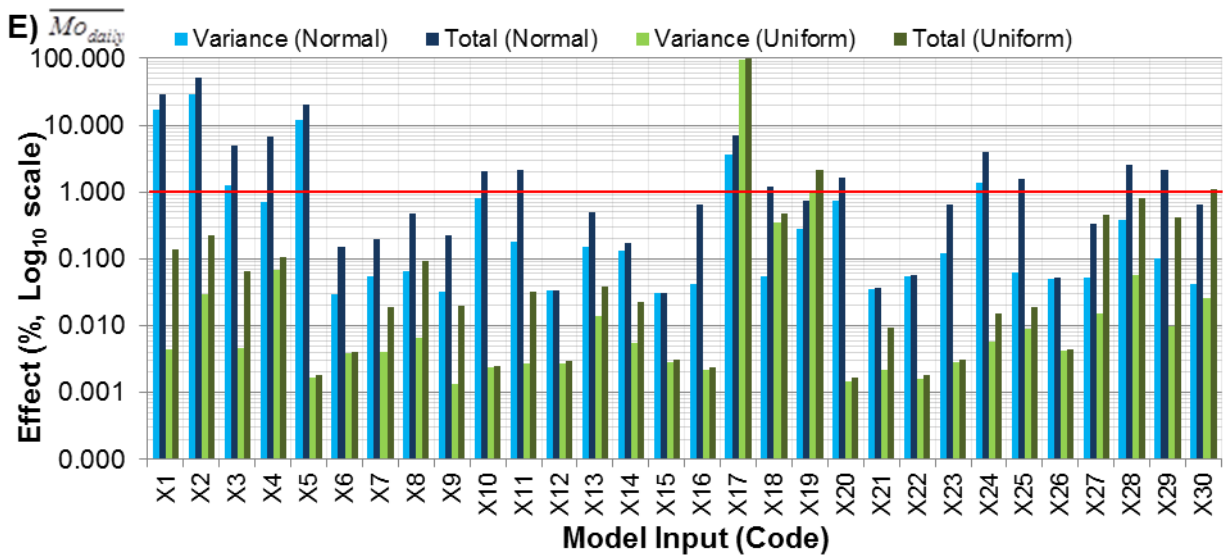
21



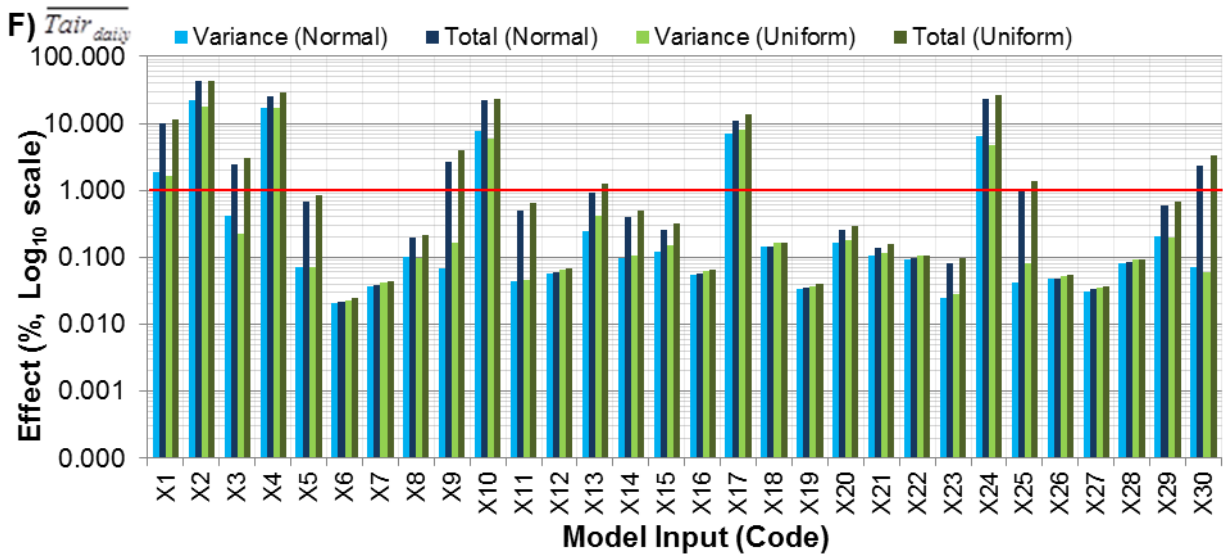
22



23

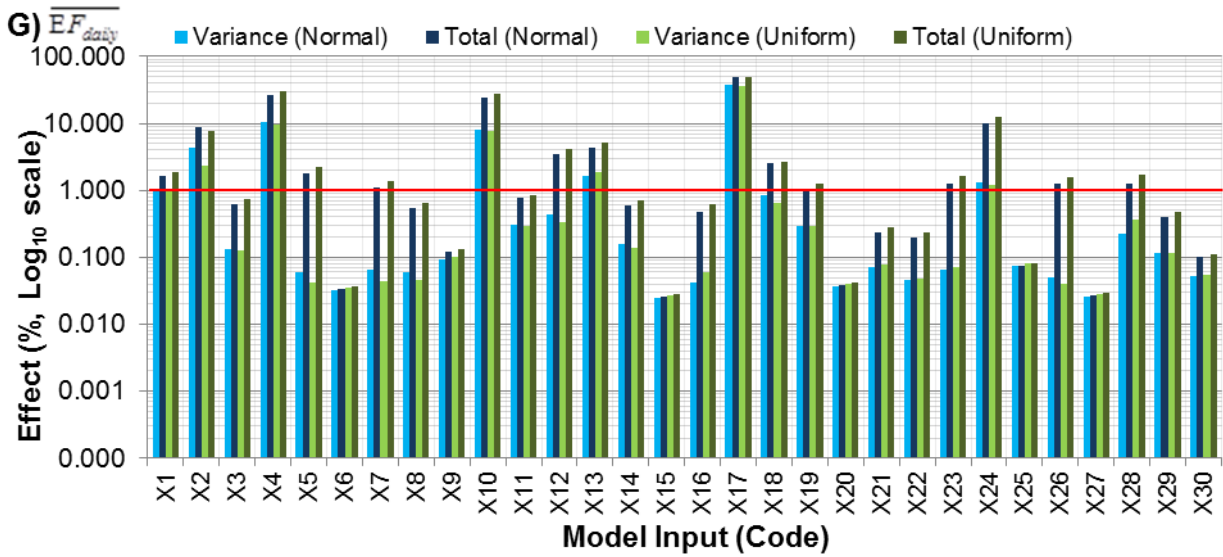


24

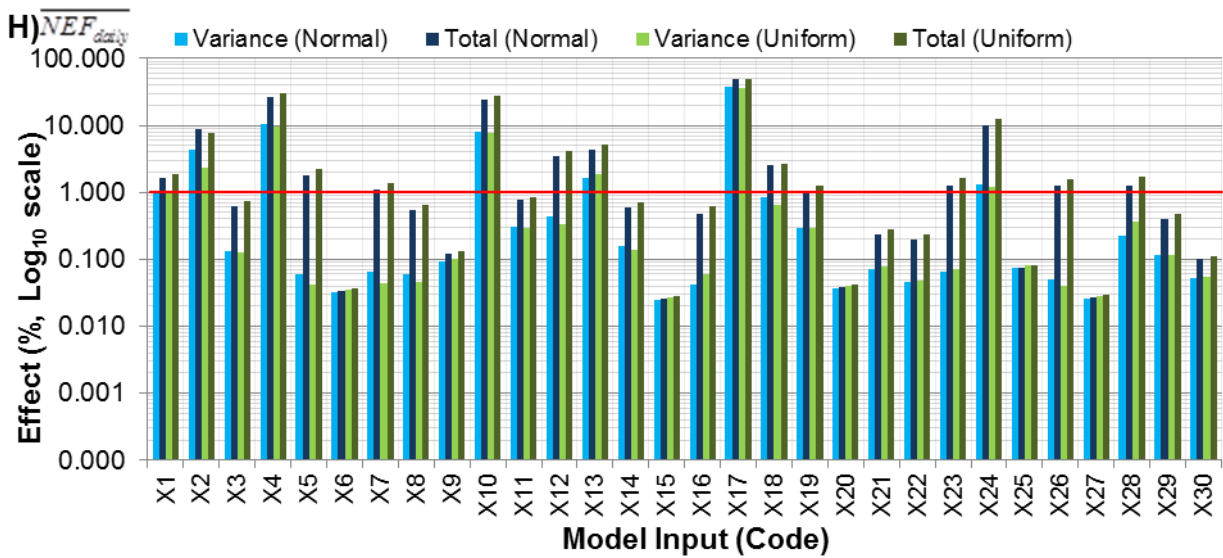


25

26



27



28

29

30 **Figure 3.** Variance Decomposition and total effects of the model inputs examined for (A)  
 31  $\overline{Rn}_{daily}$ , (B)  $\overline{H}_{daily}$ , (C)  $\overline{LE}_{daily}$ , (D)  $\overline{Trad}_{daily}$ , (E)  $\overline{Mo}_{daily}$ , (F)  $\overline{Tair}_{daily}$ , (G)  $\overline{EF}_{daily}$  and (H)  
 32  $\overline{NEF}_{daily}$ . Vertical axis is logarithmic ( $\text{Log}_{10}$ ), with the red line across the graphs at 1%  
 33 signifying those parameters that are highlighted in Tables 3 and 4.

34